Nano-patterned Hydrogel for Corneal Wound Healing

Thesis

Presented in Partial Fulfillment of the Requirements for Honors Research Distinction in

The Ohio State University

By

Shoyo Hakozaki

Undergraduate Program in Biomedical Engineering

The Ohio State University

2019

Thesis Committee

Dr. Jessica O. Winter, Advisor

Dr. Alexis Ortiz-Rosario

Abstract

Corneal wounds are the most common medical trauma treated in emergency departments. Natural corneal wound healing process can be too slow to completely heal the wound, and can lead to serious vision damage. However, current standard treatments do not actively enhance the wound healing cascade, but rather aim only to minimize pain and infection. Thus, new treatment modalities to facilitate corneal wound healing are needed for corneal wounds.

The goal of this study was to design hydrogels, which can be used to create contact lenses with nanopatterns printed on the surface to enhance corneal wound healing. Nanopatterned surfaces were selected as wound healing modalities for their known effects of promoting cell migration, proliferation, and orientation in the wound healing process. Effects of nanopatterned hydrogel lenses on *in vitro* corneal wound healing of human corneal epithelial cells (HCECs) were investigated. It was hypothesized that nanopatterned hydrogel lenses would significantly increase the wound closure rate of HCECs compared to hydrogel lenses with no pattern. Hydrogel lenses with different materials, specifically, agarose and polyetheylene glycol diacrylate (PEGDA) with nanopatterns were tested in a transwell wound healing model. HCECs were cultured as monolayers on a transwell membrane, and a gap of 500 μm was created to represent a

wound on the cornea. Nanopatterned hydrogel lenses were then layered on top of the HCECs with the patterned surface facing the cells. Wound closure was then measured by fluorescent microscopy over a 24 hour culture time.

Nanopatterned hydrogel lenses (both agarose and PEGDA) significantly improved wound closure compared to nonpatterned lenses and no lens conditions. Both agarose and PEGDA lenses, either patterned or nonpatterned, significantly enhanced wound closure compared to the no lens condition, yet PEGDA was more effective. Overall, these data successfully establish a clinically relevant model for studying corneal wound healing. Further optimization should be performed to develop nanopatterned PEGDA contact lens as the potential method for treating corneal wounds.

Acknowledgments

I would like to thank Dr. Jessica Winter, Yixiao Cui and Faiz Nisar for generously supporting me along the way as my mentors.

In addition, I would like to thank CEMAS for electron microscopy performance at the Center for Electron Microscopy and Analysis (CEMAS) at The Ohio State University, Dr. Heather Chandler for offering us human corneal epithelial cell line, and Marcos Cortes-Medina for his generous support in stiffness analysis.

I would also like to acknowledge financial support from The Ohio State University College of Engineering.

Vita

2015 to present …….. B.S. Biomedical Engineering, The Ohio State University

Fields of Study

Major Field: Biomedical Engineering

Table of Contents

List of Tables

List of Figures

Chapter 1. Introduction

Background and motivation

Corneal wounds are the most common events treated in emergency departments, and nearly 20% of the population in US suffers from an eye trauma injury in their lifetime [1]. Corneal wounds can be caused by contact with foreign bodies, abrasions, and chemical burns, and always result in disruption or removal of corneal epithelium cells [2]. Many corneal wound cases do not involve noticeable traumatic events, such as poking the surface of the eye [3, 4]. However, the simple action of scratching the eye can easily cause corneal abrasion, especially with dry eyes and small particles in the air, including sand and dust. When left untreated, corneal wounds can result in disrupted vision and increased susceptibility to bacterial infections, causing serious eye damage, up to and including permanent vision loss [5]. In addition, the natural corneal wound healing process is too slow to completely heal the wound, and sometimes this can lead to blurred vision [6]. The existing treatment options for corneal wounds aim to minimize pain and infection, often in the form of topical antibiotics, which do not specifically improve the healing process of the wound [7]. Therefore, new treatments that enhance corneal wound healing are critically needed.

In the field of nano/microtechnology, it is well known that nanotopography can enhance cell migration, proliferation and orientation, thereby improving the wound healing cascade; nanopatterns can also aid cells with securely adhering to surfaces, which supports cell migration

and orientation, as well as cell proliferation [8, 9]. Hence, the application of nanotopography on the wounded site could potentially augment the wound healing process.

Significance

Although corneal wounds are extremely common trauma events, current clinical treatments for the corneal wounds do not focus on the wound healing process, but rather aim only to minimize the pain and infection [7]. Because nanotopographies can enhance cell migration, proliferation, and orientation, application of a nanopatterned contact lens is expected to improve the wound healing process, providing a potentially simple, yet cost-effective solution. After the wound healing process, the contact lens could easily be removed from the corneal surface.

Conventionally, many wound healing assays are conducted on solid surfaces, in which cells are simply cultured on plates with the introduction of a wound gap by scratching. This is commonly known as the scratch wound assay [10]. However, this model does not accurately reflect the eye anatomy. *In vivo* epithelial cells can access medium from the eyeball via blood vessels, whereas cells in the conventional model can only access medium from their top surfaces, and not from the plate surface; this raises a problem in that, when a contact lens is applied to the conventional model, the lens and plate surface block the cells' access to medium, severely inhibiting cell activity (Figure 1). Because of this problem, this study sought to develop a wound healing model better suited for *in vitro* experimentation with contact lenses.

In this research, the nanopatterned hydrogel lenses made from agarose and poly-(ethylene glycol) diacrylate (~10k Da PEGDA) were tested using an *in vitro* corneal wound model on a

transwell insert, a porous membrane cell culture insert (Figure 1). This *in vitro* model better represents the actual human cornea compared to the conventional wound healing model [11]. The corneal cells can access the culture medium through the porous transwell membrane in this model, unlike the conventional model, which blocked medium access with hydrogel lens and the bottom plate surface.

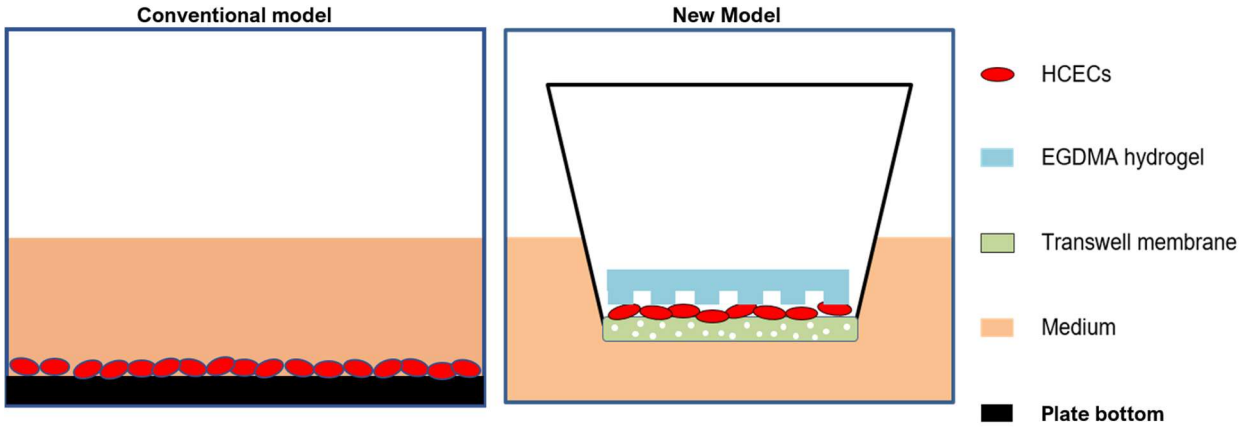

Figure 1: Conventional scratch assay and new model with the nanopatterned hydrogel lens.

Preliminary data

Prior to experimentation to evaluate the hypothesis, preliminary data were collected to evaluate the new model's validity. Based on the results and conclusion from Parikh et al. [12], a previous study in our group, ethylene glycol dimethacrylate (EGDMA) was chosen as a hydrogel lens material because of its ability to enhance cell migration and aid in wound healing. EGDMA lenses were fabricated following the methodology described in that study: 100 µl of 1 wt. %

solution of Irgacure 651 initiator in EGDMA (98%, Signa-Aldrich) was placed on a PDMS mold with nanopatterns transferred from a silicon wafer. This solution was then cured by UV light for 15 min under nitrogen gas (Supplemental 1).

Parikh et al. (2012) describes the use of argon gas to prevent reaction with oxygen in the air [12]. EGDMA does not completely cure in air and thus sometimes a portion of the EGDMA remains unsolidified. Because of limited argon supply, nitrogen gas was used for curing instead. Using nitrogen gas resulted in a solid, completely cured EGDMA lens. Thus, nitrogen gas was used for other hydrogel fabrications as well.

EGDMA lenses were placed on *in vitro* transwell models with "wound" gaps in stained cells, generating cell-free regions on the transwell to represent corneal wounds (Figure 6). Fluorescent microscope image samples with EGDMA lenses and without lenses (control) were obtained at 0, 24, and 96 hours.

The wound gap closed well in the control (without any lens) at both 24 and 96 hour time points. The gap under the EGDMA lens did not demonstrate any cell migration over the course of 96 hours (Figure 2). In addition, cells under EGDMA lenses appeared to proliferate less than the control, indicated by the relative decrease in visible cell concentration over time. This result did not change with or without nanopatterns on the EGDMA lens (not shown). Because EGDMA lenses appeared to be a non-proliferative cue, it was concluded that EGDMA is not a favorable material for this research.

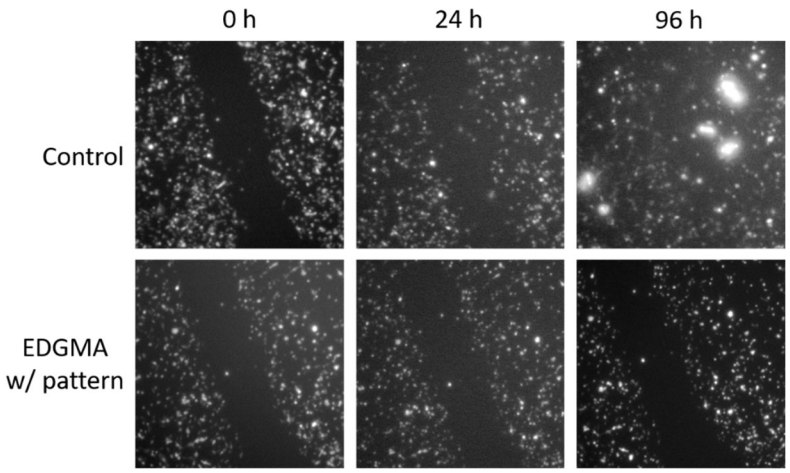

Figure 2: Preliminary cell migration study result for control and EGDMA lenses.

There were several samples that appeared to demonstrate cell gap closure under EGDMA lenses, because of “lens slip”. The acquired images illustrated distinct lines of cells at the edge of the lens, which represented the shift of the lens during/between image acquisitions (Figure 3).

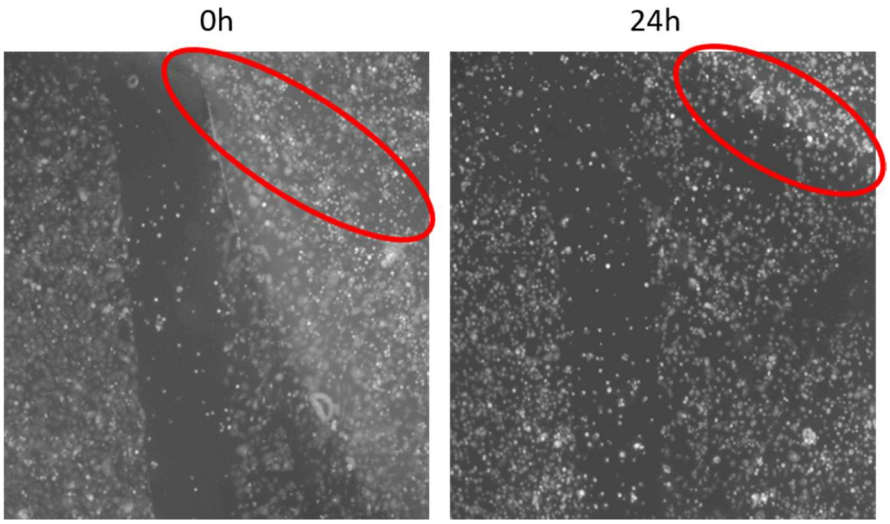

Figure 3: Lens slip creating lines of cells under EGDMA lenses.

Although the cell gaps seemed to close under EGDMA lenses under slip conditions, it was hypothesized that slip movement of the lens resulted in only passive cell movement. The EGDMA lens easily shifted around in the transwell. As the lens was half submerged in the medium placed on top of transwell membrane, the lens experienced buoyancy forces with medium acting as a lubricant. To prevent lens slip, medium on top of the transwell was aspirated out. This change resulted in a lens resistant to shift, which did not slip easily with applied impulse. Decreased slip possibly resulted from reduced buoyancy and lubrication, and increased dominancy of adhesion between transwell-medium and medium-lens. This aspiration step was applied in later experiment protocols with other hydrogels.

Hydrogel lens

Since the EGDMA lens was not suited to enhance cell migration, other types of materials were investigated as hydrogel lenses. After evaluating many criteria, including biocompatibility, stiffness to maintain shape, transparency, availability, ease of fabrication, and current application as a contact lens material, agarose and poly (ethylene glycol) diacrylate (~10k Da PEGDA) were selected as new hydrogel lens materials. Agarose is biocompatible material utilized in many cell experiments, stiff enough to maintain shape, transparent, readily available and easily fabricated into lenses [13]. PEGDA is also biocompatible, stiff, transparent, available on the market, easily fabricated into lenses, and known as a common, soft contact lens material [14] [15] [16]. In this research, nanopatterned agarose and PEGDA were used as hydrogel lens materials.

For selecting the nanopattern design to be printed on the hydrogel lens surface, several factors were considered. To begin with, the nanopattern structure must be isotropic in shape;

wound healing should be enhanced for all directions, so the nanostructure should not be directional. Cylindrical structures with an isotropic shape on 2D surfaces, were thus selected as elements of the nanopattern.

Similarly, the placement of the cylindrical structures should be isotropic. However, completely isotropic placement of finite discrete structures on 2D surfaces is not geometrically possible. In nanostructure placement, a line connecting 2 structures uniquely defines a geometric direction. The finite structure of 2D surfaces defines finite geometric directions, resulting in anisotropic pattern placement. Anisotropy can be minimized by placing structures in random locations, which averages out the geometric directions between pattern structures, resulting in negligible anisotropy. Nevertheless, randomly placed structures can be difficult to characterize. When confirming the success of the printing nanopatterns into hydrogels, randomized structure placement would be challenging to objectively evaluate. Because completely anisotropic or randomized structure placements are not practical, a rectangular matrix placement was selected. Rectangular matrices on 2D surfaces can easily be characterized by measuring dimensions with 2 dominant directionalities, orthogonal to each other, expected. Therefore, nanostructure placement was chosen to consist of 2D rectangular matrices spaced apart by the same distance in both x and y directions (Figure 4).

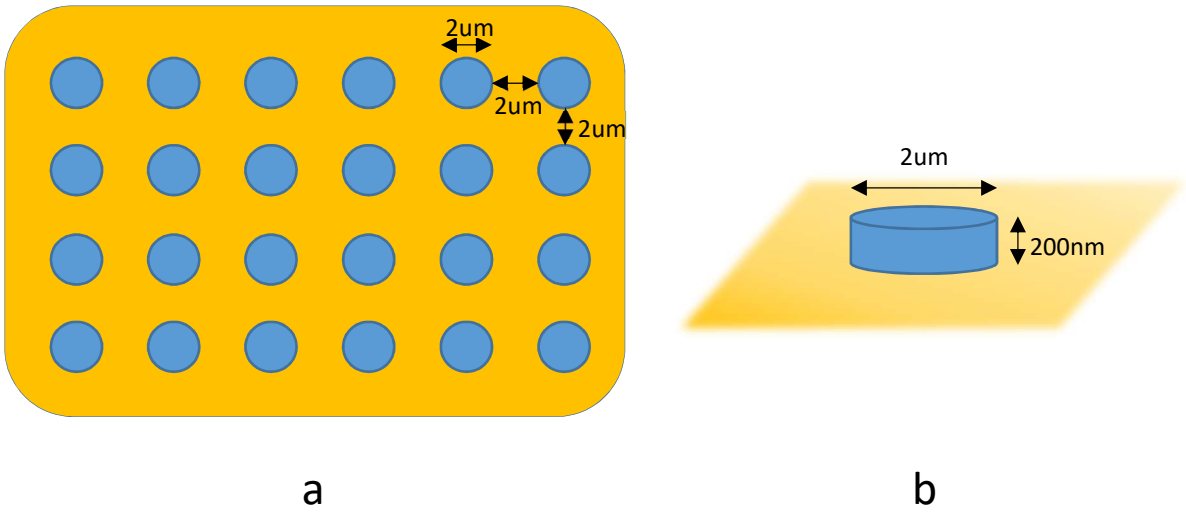

Figure 4: Design of the nano-patterns. a) Magnified orientation and dimensions of the cylinder matrix patterns. b) 3D view of the nano-cylinder.

Chapter 2. Methodology

HCEC culture

Human corneal epithelial cells (HCECs, Dr. Chandler lab) were cultured in an incubator at 37℃ with 5% CO_2 atmosphere, using KGM culture medium; TM Gold Keratinocyte Growth Basal Medium (KGM, Lonza) was supplemented with 10% fetal bovine serum and 1% penicillin and was filtered through a 0.22 μm filter (Stericup and Steritop vacuum driven disposable bottle top filter, Sigma-Aldrich) into autoclaved bottles. HCECs were housed in 25 cm^2 tissue culture flasks (VMR) with 8ml KGM medium. Culture medium was changed 2 times per week, and cells were passaged weekly at confluence prior to use. For passaging, medium was completely aspirated from the flask and the flask was rinsed with warm phosphate buffered saline (PBS), followed by 2ml warm 0.25% trypsin in PBS. Flasks were incubated at 37℃ for 5-10 min, and when the cells were detached from the flask surface, 8ml KGM medium was added. The mixture was then transferred to a 15ml conical tube and centrifuged at 2400 rpm for 10 min at 4℃. Supernatant medium was aspirated, and precipitated cells were resuspended in 1ml KGM medium. Cells were counted using a hemocytometer and 500,000 cells were transferred to new flask with 8ml KGM medium. Remaining cells were transferred to freezing vials (500,000 cells/vial) in 1ml KGM medium and 50 μl DMSO. Cells in vials were slowly cooled to -80℃ in ethanol cylinder. After 24 hours, the vials were stored in -80℃ or liquid nitrogen for later use.

Nanotopography design and fabrication

The nanotopography pattern was composed of small cylinders, 2000 nm in diameter and 200 nm in height, which were spaced apart (pitch) by 2000 nm in a 2D matrix on a flat surface (Figure 4).

A silicon wafer master was fabricated using electron beam lithography with the designed nanopattern. The pattern on the wafer was transferred to polydimethylsiloxane (PDMS) gels by pouring mixture of Sylgard 184 Silicon Elastomer Base (Sigma-Aldrich) and 10% Sylgard 184 Silicon Elastomer Curing Agent (Sigma-Aldrich) onto the wafer surface. Bubbles in the PDMS were removed by applying multiple vacuum cycles. The patterned PDMS then was cured at 60 ℃ for 2 hours.

The PDMS pattern was then transferred to agarose and PEGDA hydrogels. For agarose gel fabrication, 4.0 wt. % solution of agarose in water was heated at 90℃ for 5 min for dissolution and bubble removal. Then, 100 µl of the agarose solution was cooled on the patterned PDMS surface as a hemispherical droplet at room temperature for 15 min. For PEGDA fabrication, 15 wt. % of PEGDA (Sigma-Aldrich) and 3 wt.% of photo-initiator (2,2-Dimethoxy-2-phenylacetophenone, Sigma-Aldrich) solution in water was heated at 60℃ for dissolution. Then, 100 µl of the PEGDA solution was placed on the patterned PDMS surface to form a hemispherical droplet [17]. The PEGDA sample was then cured by UV light for 20 min under nitrogen gas. After solidification, the hydrogels were carefully peeled from the PDMS template (Figure 5).

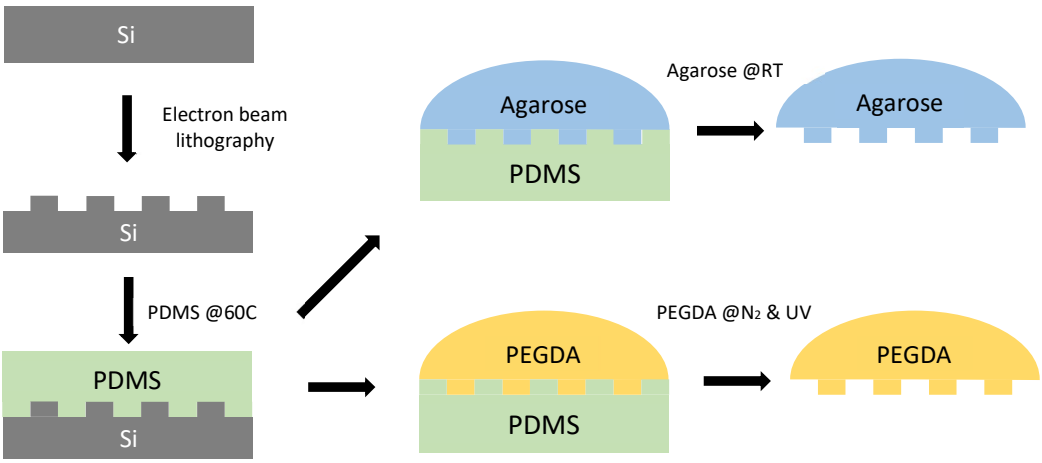

Figure 5: Schematic diagram of the pattern transfer and hydrogel fabrication.

Hydrogel characterization

Separate from the corneal wound healing assay, hydrogels were characterized to quantify their properties. Hydrogel samples were observed under light microscopy to ascertain any potential interference pattern from structural coloration, which would be evidence of successful patterning. For scanning electron microscopy (SEM) imaging, 4 samples were prepared: 2 agarose and 2 PEGDA gels, 0 day and 1 day post fabrication, respectively. For 1 day post fabrication hydrogels, they were submerged in PBS for 24 hours. Hydrogels were dehydrated with a graded series of ethanol solutions in DI water (50, 70, 80, 95 and 100% ethanol) each for 5 min, followed by graded solutions of hexamethyldisiloxane (HMDS, Sigma-Aldrich) in ethanol (25, 50, 75 and 100% HMDS) for imaging. Dehydrated hydrogel samples were then mounted on sample holders with conductive carbon paint to securely maintain the patterned surface facing up, gold coated and observed under SEM.

Hydrogels samples were also tested for stiffness using an RSA-III dynamic mechanical analyzer. The samples were compressed vertically with an applied strain of 10% and based on the stress value and contact lens dimensions, elastic modulus values were calculated [18].

Corneal wound healing assay

For model preparation, medium was thoroughly aspirated from flasks and cells rinsed with warm PBS, followed by 2ml warm 0.25% trypsin. Flasks were incubated at 37℃ for 5-10 min. KGM medium (8 ml) was added when the cells detached from the flask surface. The mixture was then transferred to a 15ml conical tube and centrifuged at 2400 rpm for 10min at 4℃. Supernatant medium was aspirated, and precipitated cells were resuspended in 1ml KGM medium. Cells were counted using a hemocytometer, and 500,000 cells were suspended in 1ml KGM medium with 1 µl cell tracker (CellTracker^{TM} Green CMFDA, Thermo Fisher Scientific). After 45 min incubation at 37℃, the suspension was centrifuged; the supernatant was aspirated; and cell precipitates were re-suspended in 1 ml KGM medium, creating a 500,000 cells/ml suspension.

iBidi 2-chambered inserts (ibidi) were rinsed with 70% ethanol and air dried for 1 hour. The inserts were then securely attached to the membrane in transwells (VMR) by gently pressing against the membrane, ensuring no gaps or air bubbles were present at the interface. Transwells were placed in 12-well plates (VMR) and 70 µl of 500,000 cells/ml suspension was added into each chamber space. Plates were incubated for 24 hours at 37℃. After incubation, 1ml KGM medium was added to the wells, and the inserts were gently removed from the transwell, leaving

500 µm “wound” gaps (Figure 6). To prevent lenses from floating and to maintain cell-free gaps, transwell surfaces were gently rinsed with KGM medium, and remaining medium on the transwell was removed by pipette. Fabricated hydrogel lenses were carefully placed on top of prepared transwell membranes with the nonpatterned (plain flat) or patterned surface facing down.

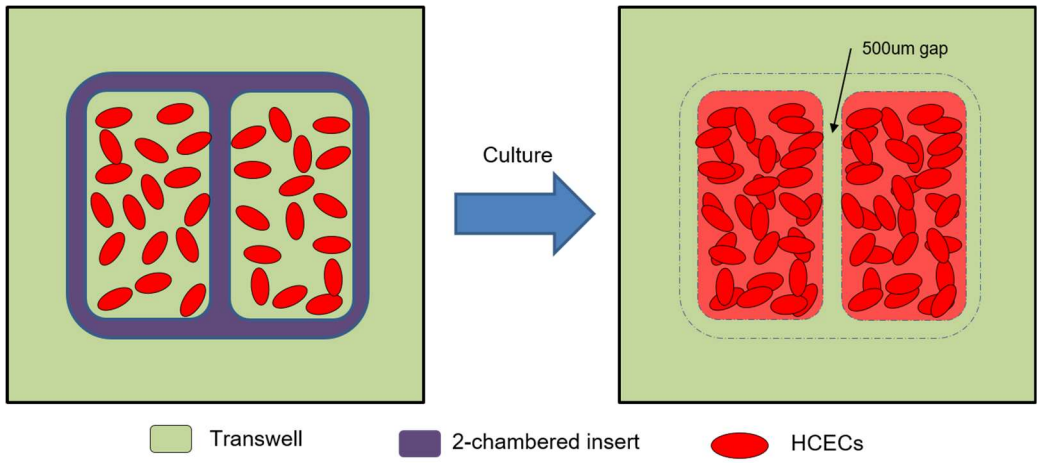

Figure 6: Formation of the in vitro corneal model on transwell with 500 µm-wide “wound”.

Fluorescent microscopy

Plates were imaged with a fluorescent microscope at 40x magnification using FITC filter and MicroMorph Basic software. The stage coordinates for all locations of the patterned/center region of the hydrogel lenses were identified and marked using the multistage function. Images of the samples were acquired at 0 hour and 24 hours post placements of hydrogel lenses on the transwell membranes.

Image data analysis

For each image, areas of the gap regions (the cell-free region established between the 2 chambers) were quantified using ImageJ (NIH) by manually setting the gap boundary lines. The wound closure percentages were then calculated based on the equation below (Equation 1), where $A_{t=0}$ and $A_{t=24}$ are the areas of gap regions at 0 and 24 hours, respectively.

$$\%\, Wound\ Closure = \frac{A_{t=0} - A_{t=24}}{A_{t=0}} * 100\% \qquad \text{Equation 1}$$

The wound closure percentages for each condition (control, agarose with pattern, agarose without pattern, PEGDA with pattern, PEGDA without pattern) were analyzed using JMP statistical software (SAS). One-way ANOVA, followed by the Tukey-Kramer HSD post hoc test were conducted to identify any statistically significant difference between the conditions. The data were also analyzed using the control Dunnett's test to compare each condition against the control. All analyses were conducted at a significance level (α) of 0.05.

Chapter 3. Result

Hydrogel fabrication and characterization

Patterned silicon wafers were successfully fabricated using electron beam lithography and patterns were transferred to PDMS. The interference pattern observed on the nanopatterned surface because of light diffraction served as an indication of the presence of nano/micro size structures. (Figure 7).

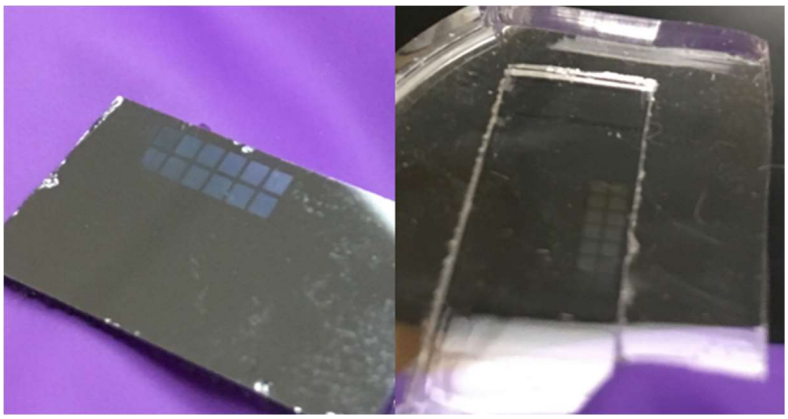

Figure 7: Interference pattern on silicon wafer (left) and PDMS mold (right) indicating nanoscale features.

The fabricated hydrogels, both agarose and PEGDA maintained a hemispherical contact-lens-shape after curing, displaying enough stiffness to maintain shape outside of culture medium. Agarose lenses were transparent with light blue opaqueness, whereas PEGDA lenses were transparent with yellow-orange coloring (Figure 8). Interference color patterns were visible by the naked eyes on both hydrogels and subsequently identified under brightfield microscopy,

indicating the presence of nanopatterning (Figure 9). The hydrogels were mostly debris free except for a few dust particles and air bubbles (Figure 9).

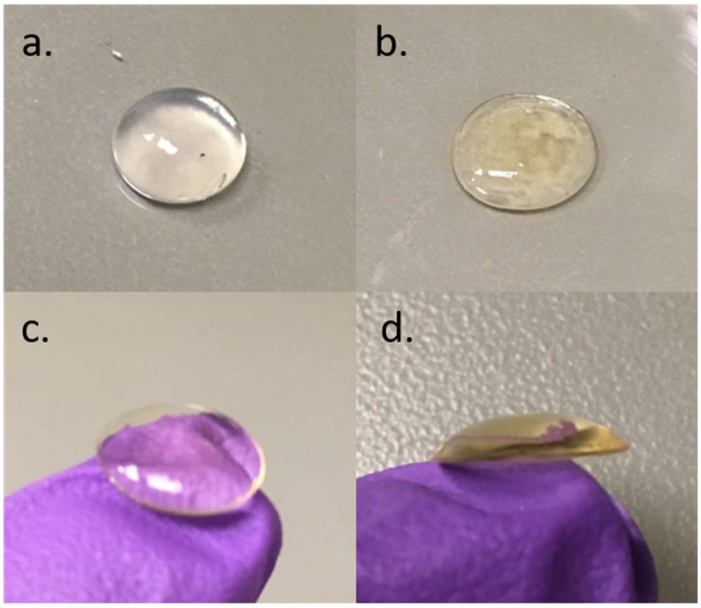

Figure 8: Hydrogel samples: a) agarose, b) PEGDA, c) PEGDA maintaining shape in air, and d) PEGDA displaying hemispherical lens shape.

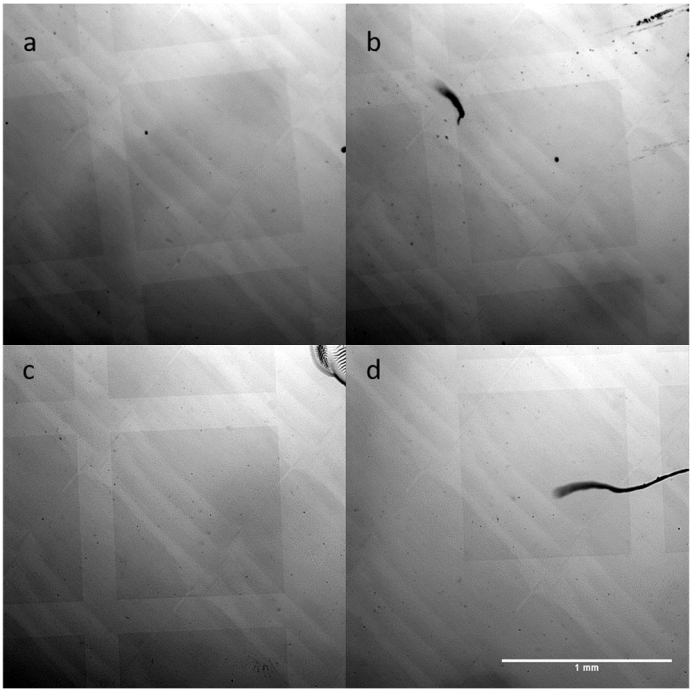

Figure 9: Interference patterns in square shapes: a) agarose, b) agarose with debris/bubble, c) PEGDA, and d) PEGDA with debris.

For SEM imaging, hydrogels were dehydrated with graded solution of ethanol and HDMS. However, during HDMS dehydration, both PEGDA and agar hydrogels shrunk, as the water content in the hydrogels were removed. Agarose shrinkage mainly occurred in the vertical direction (height) and did not change significantly in the horizontal direction (width). Agarose remained transparent and became extremely stiff. On the other hand, PEGDA hydrogels shrunk significantly to less than half their original diameter, with severe edge curls toward the flat surface. PEGDA also displayed whitening on the edges, developed an opaque yellow cluster in the center, and became stiff (Figure 10).

Figure 10: Dehydrated hydrogels, agarose (right) and PEGDA (left).

SEMs of PEGDA hydrogels illustrated the highly disturbed surface with numerous cracks and clustering. Both 0 day and 1 day old PEGDA hydrogels were highly distorted. The surfaces were not uniformly disturbed, but rather had chaotic combinations of cracks and clustering, resulting in non-uniform deformation patterns. The edges and center of the flat surfaces appeared

to have a sponge-like structure, with a network of dried fabric/membrane structures. The center of the surface consisted of mountain-like structures, in addition to a smooth, gradual gradient spongy structure observed in the area. Sizes of the surface distortion structures were significantly bigger than the printed nanopattern structures. There was no evidence of nano-size cylindrical structures found on the PEGDA surface on either 0 day and 1 day old samples, possibly because of the dehydration process (Figure 11).

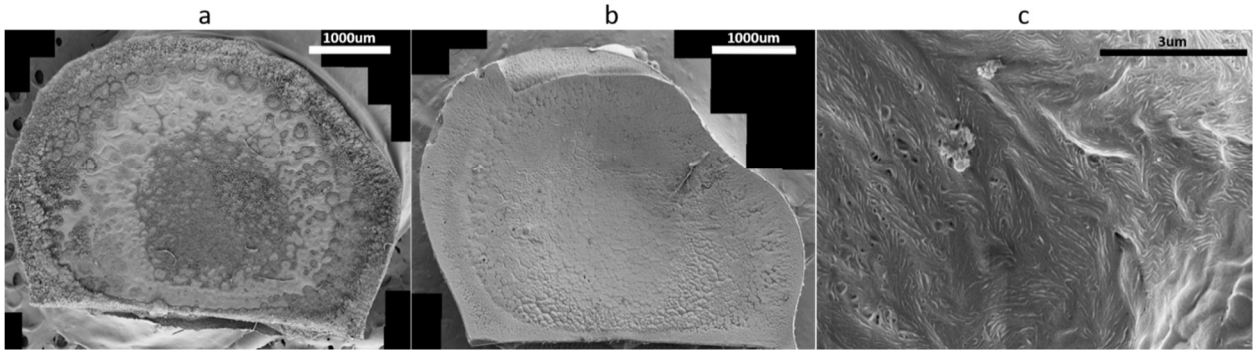

Figure 11: SEM images of PEGDA hydrogels: a) 0 days, b) 1days, and c) magnified surface of 1 days.

SEMs of agarose hydrogel displayed cleaner, undisturbed surfaces, with nanopatterned cylindrical structures observed. The dimensions of the patterns were measured to be 2.00 μm in diameter and 2.00 μm apart (pitch) from each other in x and y directions. Although some debris, misprints and deformations were observed, most of the patterned surfaces remained undistorted. There was no apparent difference between 0 day and 1 day old samples, as they both displayed relatively clean surfaces with clearly observable cylindrical patterns (Figure 12).

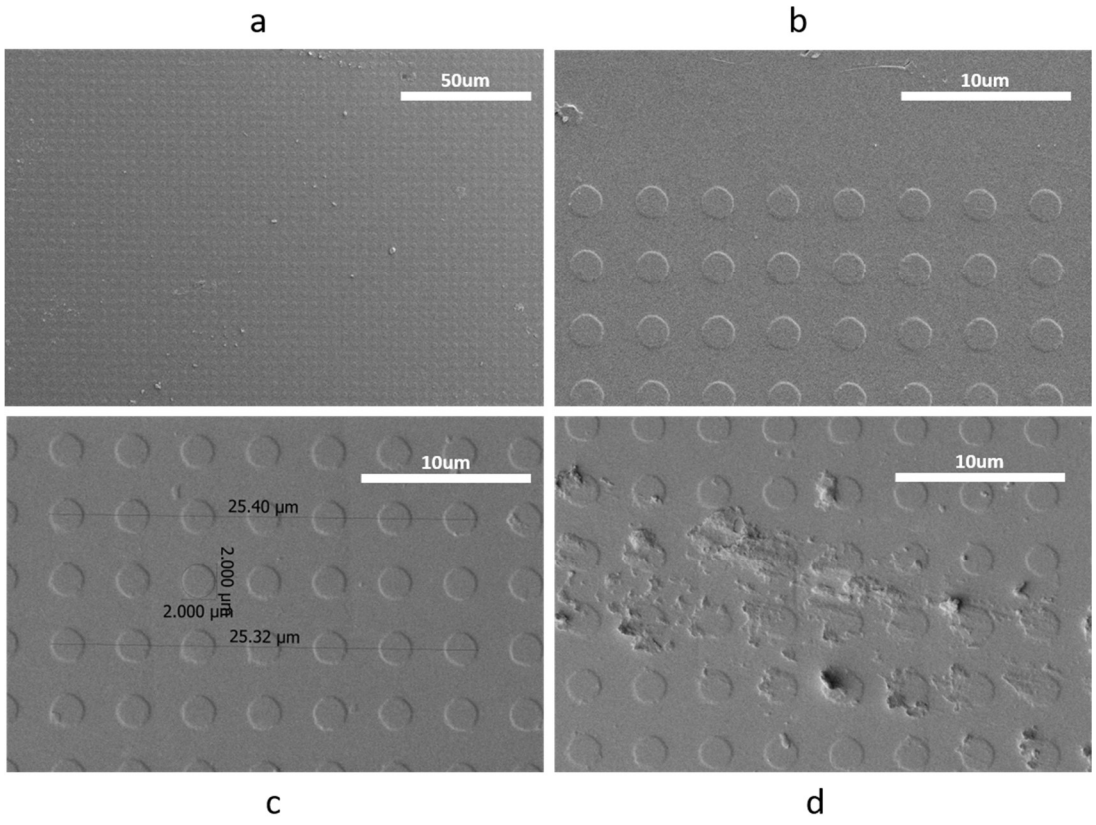

Figure 12: SEM images of agarose: a) wide-field view of 0 days, b) 0 days, c) 1 days with dimensions, and d) deformed surface (1 days).

For the stiffness test, the elastic modulus for agarose hydrogels was 10.87 ± 1.56 kPa (n = 4) and for PEGDA hydrogels was 54.49 ± 18.50 kPa (n = 5). Thus, PEGDA demonstrated higher stiffness compared to agarose hydrogels, yet also had more variance per sample (Figure 13).

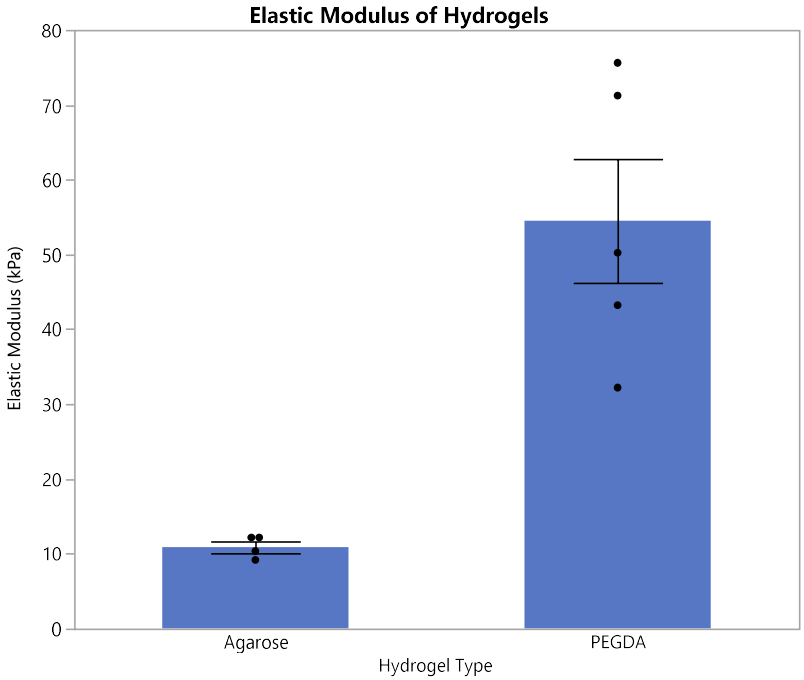

Figure 13: Elastic modulus values of agarose (n = 4) and PEGDA (n = 5). Each error bar represents 1 standard error from the mean.

Corneal wound healing assay

Wound healing assays were conducted with 6 samples per condition, and assays were performed on 3 separate different days to minimize the effect of confounding variables. When imaged at 0 hours, if the cell gap was disrupted or was not well established, the sample was excluded from the study; cell gap was considered disrupted if there were cell clusters present in gap region in the 0 hour image, which should be clear of cells at this initial state. Lens slippage indicated as distinct lines of cells was not observed, indicating that the hydrogel lenses did not slipp on the transwell. Although the stage coordinates were recorded in the imaging software, some images from the same samples appeared to have translated or rotated slightly over the 24

observation hour time. Nonetheless, these shifts were minimal and did not influence image analysis

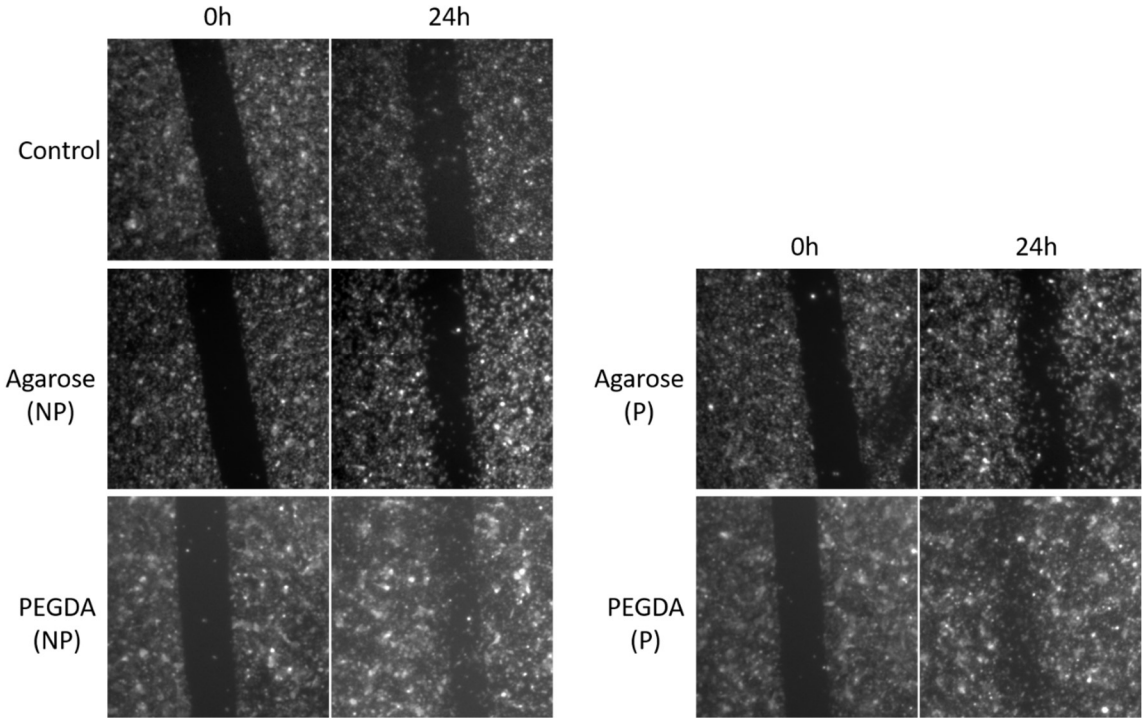

Figure 14: Example images from the wound healing study for experimental and control conditions. NP = non-patterned, P = patterned. Control consisted of no hydrogel.

As shown above, the wounds closed to some extent in all conditions: control, agarose without pattern (NP), agarose with pattern (P), PEGDA without pattern (NP) and PEGDA with pattern (P) (Figure 14). Wounds seemed to close best for PEGDA lens samples, followed by agarose lenses, and the control condition. After image analysis, wound closure percentages were calculated to be 3.5 ± 4.3 % for control, 19.5 ± 5.0 % for agarose (NP), 32.8 ± 8.3 % for agarose (P), 64.0 ± 11.6 % for PEGDA (NP) and 83.8 ± 14.9 % for PEGDA (P) (Table 1) (Figure 15).

Table 1: Result of the wound closure assay for each experimental condition (n=6 for each condition)

Conditions	% Closure	
	Mean	STD
Control	3.5	4.3
Agarose (NP)	32.8	8.3
Agarose (P)	19.5	5.0
PEGDA (NP)	64.0	11.6
PEGDA (P)	83.8	14.9

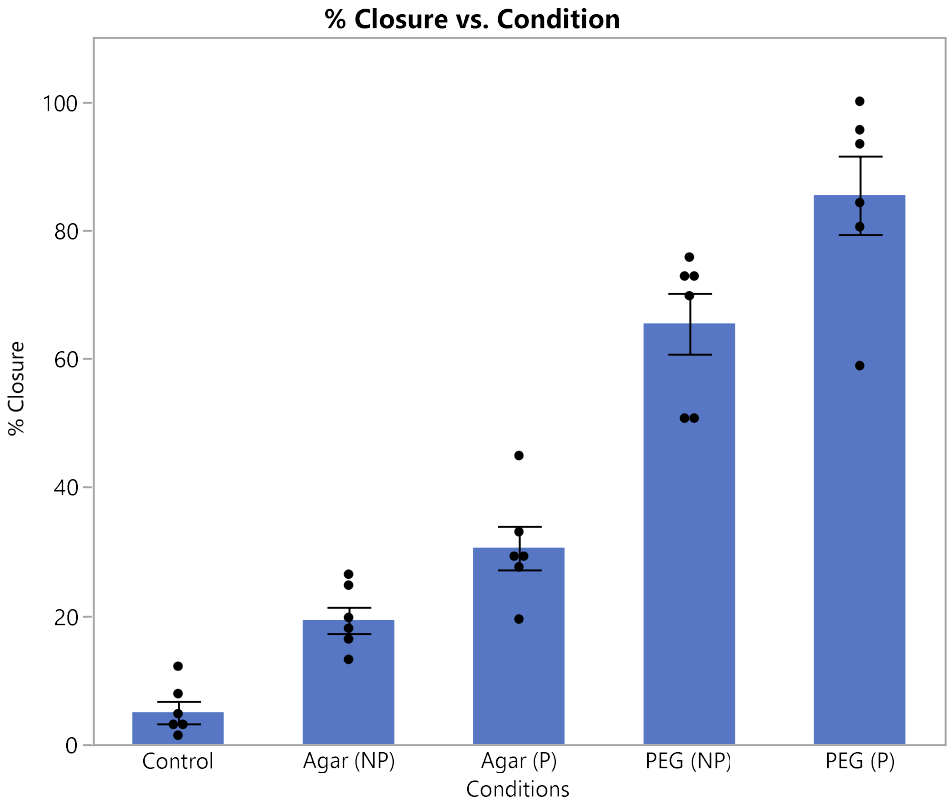

Figure 15: Percent wound closure with standard errors for all conditions (n = 6 each). Each error bar represents 1 standard error from the mean.

Data were then evaluated for statistical significance using ANOVA. Before conducting ANOVA, the validity of the normal distribution and equal variance assumptions were evaluated (Supplemental 3). Both assumptions were valid, indicating the appropriateness of the use of ANOVA. One-way ANOVA resulted in p-value < 0.0001, which indicated at least one significant difference between the means of each condition. The Tukey-Kramer test was then used as the post hoc test (Supplemental 4). Of all conditions, agarose (P), PEGDA (NP) and PEGDA (P) demonstrated statistically significant difference from the control ($p < 0.05$); and agarose (NP) showed a notable, though not significant difference, according to the selected alpha value and N of this experiment ($p = 0.1074$). Moreover, there were statistically significant difference between PEGDA (P) and PEGDA (NP), PEGDA (NP) and agarose (NP), and PEGDA (P) and agarose (P). Similar results were obtained using the control Dunnett's test, further supporting these conclusion (Supplemental 5).

Chapter 4. Discussion

Fabricated agarose and PEGDA lenses demonstrated sufficient stiffness to maintain their shape in the air, while possessing some elasticity (Figure 8). Moreover, both agarose and PEGDA lenses were transparent with limited opaqueness. Although there was some debris and air bubbles observed via brightfield microscopy, lenses were mostly uniform. Since the lenses were generally free of defects and maintained pattern transfer, the effect of debris and bubbles on wound healing closure was anticipated to be minimal. Because elasticity, ability to maintain shape, transparency and uniform fabrication processes are essential for the possible future application as a soft contact lens, the fabricated lenses demonstrated successful characteristics.

Silicon wafers, PDMS molds, and hydrogel lenses (agarose and PEGDA) demonstrated square-shaped interference patterns (Figure 7) (Figure 9). Interference patterns occur when nano/micro-size patterns on surfaces interact with lights, causing a unique color-patterned reflection, known as structural coloration [19, 20]. The presence of these interference patterns indirectly implied the success of pattern transfer, as interference patterns are likely to be caused by the nanopatterns printed on the lens surfaces.

During the dehydration process for SEM imaging, the PEGDA hydrogel experienced severe shrinkage, as these are mostly composed of water (~80%). Dehydration disturbed the surface extensively with only relatively large wrinkles and cracks observed on the surface, leaving no hint of nanopatterns (Figure 11). Therefore, the presence of the nanopatterns on PEGDA lenses could not be directly confirmed via SEM imaging.

On the other hand, the patterned surface of agarose lenses was affected less by the dehydration process. Similar to PEGDA, agarose lenses are mostly water (~96%). Nevertheless, the agarose lens did not shrink horizontally but rather, only in the vertical direction, reducing its height and leaving the patterned surface undisturbed. SEM images directly confirmed the presence of the nanopatterns on agarose lens, with measured dimensions of 2.00 μm diameter and 2.00 μm apart (pitch) in x and y directions (Figure 12). This measurement perfectly matched the original design of the nanotopography, proving successful pattern transfers from silicon wafers to PDMS to agarose lenses. Although there was some deformation on the surface, possibly caused by debris attachment, pattern misprints, and/or post-print deformations, most surfaces appeared clean, clearly expressing the cylindrical pattern. It is possible that the hydrogel lenses and their patterns might deform or degrade over the 24-hour culture time because of swelling and/or dehydration. Nonetheless, the nanopatterns were observed on both 0 days and 1 days post fabrication with no apparent differences, suggesting that nanopatterns were not significantly affected at the 24-hour time point. Because of this, it can be assumed that the nanopatterns on the agarose lens were maintained during the wound healing assay.

The interference pattern observed under brightfield microscopy indirectly suggests the presence of the nanopatterns on the PEGDA surface (Figure 9). In addition, there was a significant difference in wound closure between PEGDA with and without patterning (Supplemental 4). Because the presence of the nanopattern was the only varied factor, it can be inferred that nanopatterns were present on PEGDA, or at least were physically present in a form sufficient to cause a significant difference in wound closure. Hence, although there was no direct

evidence to prove the presence of nanopatterns on the PEGDA, it is likely that the patterns were successfully printed based on the indirect evidences.

In order to standardize the initial conditions at 0 hours, samples with disrupted cell gaps were excluded from the study; when cell clusters were observed between a cell gap in imaging at 0 hour, the cell gap was considered disrupted and discarded. Cells should be clear from the gap region at the initial state. No images were found with distinct lines of cells, indicating that the hydrogels did not slip on the transwell inserts during experiments. Therefore, lens slipping probably did not contribute to cell migration. Some images appeared to have translated or rotated slightly over time, though the images were acquired from the same stage coordinates. Theoretically, translational shift should not influence the calculation of gap area as long as the 2 images have captured similar gap regions. Rotational shift would cause greater error in gap area calculation; nevertheless, rotational shifts were minimal ($< 5°$) and did not appear to affect image analysis.

As shown in Figure 15, PEGDA (P) demonstrated the highest closure percentage, followed by PEGDA (NP), agarose (P), agarose (NP) and finally the control. Based on the ANOVA followed by the Tukey-Kramer test, agarose (P), PEGDA (NP) and PEGDA (P) displayed statistically significant differences from the control ($p < 0.05$) and agarose (NP) indicated notable, but not statistically significant, difference ($p = 0.1074$) (Supplemental 4). Similarly, the control Dunnett's test yielded significant differences for (P), PEGDA (NP) and PEGDA (P) compared to the control ($p < 0.05$), and agarose (NP) had a notable difference ($p = 0.0545$) (Supplemental 5). These data indicate that all conditions with hydrogel lenses, even those without nanopatterns, yielded higher wound closure rates than the control condition

without lenses. Thus, application of any hydrogel lens can enhance the wound healing process, compared to the wounds without lenses applied.

The significance between the PEGDA (P) and PEGDA (NP) conditions clearly illustrates that, for PEGDA, nanopatterned surfaces enhanced wound closure compared to nonpatterned surfaces. Because the presence of nanopattern was the only varied factor, this data indicates that nanopatterns on PEGDA successfully enhanced cell migration. Simultaneously, given that the presence of nanopattern was the only varied factor and there was significant difference of wound closure between PEGDA (P) and (NP), it can be further inferred that the nanopatterns were successfully transferred onto PEGDA, or at least were physically present in some form.

The significant difference observed between PEGDA (NP) and agarose (NP) lenses indicates that wound closure for PEGDA was significantly higher than that of agarose without any pattern present. Similarly, the significance between PEGDA (P) and agarose (P) demonstrates that wound closed more on PEGDA than agarose with nanopatterns. In both cases, the wound closure of PEGDA was significantly higher than that of agarose, either with or without the nanopattern printed. These differences suggest that PEGDA is better candidate hydrogel for contact lens materials for corneal wound healing. Although there are many variables that may have caused this difference in wound closure rate, including monomer size and chemical composition, one possibility is the difference in stiffness. Adhesive spreading and migration of cells correlate broadly with the effective stiffness of materials and tissues [21], indicating the possibility of cells migrating faster on stiffer PEGDA than softer agarose lenses. In addition, difference in stiffness could have caused potential difference in pattern transfer qualities, which can also result in the difference in wound closure.

Although the mean value of the wound closure percentage for agarose (P) was higher than that of agarose (NP), there was no statistically significant difference, indicating that the wound closure of agarose with pattern was not significantly higher than that of agarose without pattern. Nevertheless, p-value of 0.2900 is on the lower side and statistical difference might possibly be detected with an increased number of trials. Therefore, more experiment trials should be performed to more accurately validate the effect of nanopatterns in agarose hydrogels.

Chapter 5. Conclusion and Future Directions

In this research, an *in vitro* corneal wound healing model was developed to investigate the effect of nanopatterned hydrogel lenses on corneal wound healing. It was hypothesized that nanopatterned hydrogel lenses would significantly increase the wound closure rate of corneal cells compared to hydrogel lenses with no patterns and the control condition without any lens. Nanopatterned agarose and PEGDA lenses significantly enhanced wound closure. Interestingly, PEGDA lenses without patterns also significantly enhanced the wound closure compared to the control condition. Moreover, whether patterned or non-patterned, PEGDA lenses demonstrated more wound closure compared to agarose hydrogel lenses. Nanopatterns on agarose were confirmed under SEM, and multiple indirect pieces of evidence supported the presence of nanopatterns on PEGDA.

For future work, nanopatterns on PEGDA should be characterized under environmental scanning electron microscope (ESEM), *in situ* without the need for any dehydration process. The direct confirmation of the nanopatterns on PEGDA surfaces would more firmly support the results of this study. Moreover, further experiments with the increased number of trials should be performed to accurately validate these results. In addition, this study contains many variables that could be optimized, including lens material, hydrogel stiffness, nanopattern design, surface modification, and inclusion of porous structures enhance nutrient exchange. Those parameters should be explored in future studies to maximize enhancement of corneal wound healing. Toward clinical application for corneal wound healing, experiments should be performed not only *in vitro* but also *in vivo*, including animal experimentation, possibly using dogs, and ultimately in human subjects.

Bibliography

1. Wilson, S.E., et al., *The Corneal Wound Healing Response:: Cytokine-mediated Interaction of the Epithelium, Stroma, and Inflammatory Cells.* Progress in Retinal and Eye Research, 2001. **20**(5): p. 625-637.
2. Browner, E.A., *Corneal Abrasions.* Pediatrics in Review, 2012. **33**(6): p. 285.
3. Kirkpatrick, J.N.P., H.B. Hoh, and S.D. Cook, *No eye pad for corneal abrasion.* Eye, 1993. **7**: p. 468.
4. Patterson, J., et al., *Eye patch treatment for the pain of corneal abrasion.* Southern medical journal, 1996. **89**(2): p. 227-229.
5. Kaiser, P.K., *A Comparison of Pressure Patching versus No Patching for Corneal Abrasions due to Trauma or Foreign Body Removal.* Ophthalmology, 1995. **102**(12): p. 1936-1942.
6. Eke, T., D.A. Morrison, and D.J. Austin, *Recurrent symptoms following traumatic corneal abrasion: Prevalence, severity, and the effect of a simple regimen of prophylaxis.* Eye, 1999. **13**: p. 345.
7. Wilson, S.A. and A. Last, *Management of corneal abrasions.* Am Fam Physician, 2004. **70**(1): p. 123-8.
8. Flemming, R.G., et al., *Effects of synthetic micro- and nano-structured surfaces on cell behavior.* Biomaterials, 1999. **20**(6): p. 573-88.
9. Dua, H.S. and J.V. Forrester, *Clinical Patterns of Corneal Epithelial Wound Healing.* American Journal of Ophthalmology, 1987. **104**(5): p. 481-489.
10. Cory, G., *Scratch-wound assay.* Methods Mol Biol, 2011. **769**: p. 25-30.
11. Justus, C.R., et al., *In vitro cell migration and invasion assays.* Journal of visualized experiments : JoVE, 2014(88): p. 51046.
12. Parikh, K.S., et al., *Ceramic nanopatterned surfaces to explore the effects of nanotopography on cell attachment.* Materials Science and Engineering C, Biomimetic Materials, Sensors and Systems, 2012. **32**(8): p. 2469-2475.
13. Heit, B. and P. Kubes, *Measuring Chemotaxis and Chemokinesis: The Under-Agarose Cell Migration Assay.* Science's STKE, 2003. **2003**(170): p. pl5.
14. Nemir, S., H.N. Hayenga, and J.L. West, *PEGDA hydrogels with patterned elasticity: Novel tools for the study of cell response to substrate rigidity.* Biotechnology and Bioengineering, 2010. **105**(3): p. 636-644.
15. Johnston, F.E.G.W., *Polyurethane diacrylate compositions useful for contact lenses and the like*. 1982, Tyndale Plains-Hunter Ltd: USA.
16. Froix, M., *Clouding-resistant contact lens compositions*. 1988: USA.
17. Davis, N., *Polymeric Drug Delivery Techniques: Translating Polymer Science for Drug Delivery*. 2019, Sigma-Aldrich.

18. Rennerfeldt, D.A., et al., *Tuning mechanical performance of poly(ethylene glycol) and agarose interpenetrating network hydrogels for cartilage tissue engineering.* Biomaterials, 2013. **34**(33): p. 8241-57.
19. Gu, Z.-Z., et al., *Structural Color and the Lotus Effect.* Angewandte Chemie International Edition, 2003. **42**(8): p. 894-897.
20. Shevtsova, E., et al., *Stable structural color patterns displayed on transparent insect wings.* Proceedings of the National Academy of Sciences, 2011. **108**(2): p. 668.
21. Engler, A.J., et al., *Surface probe measurements of the elasticity of sectioned tissue, thin gels and polyelectrolyte multilayer films: Correlations between substrate stiffness and cell adhesion.* Surface Science, 2004. **570**(1): p. 142-154.

Appendix A. Supplemental Data

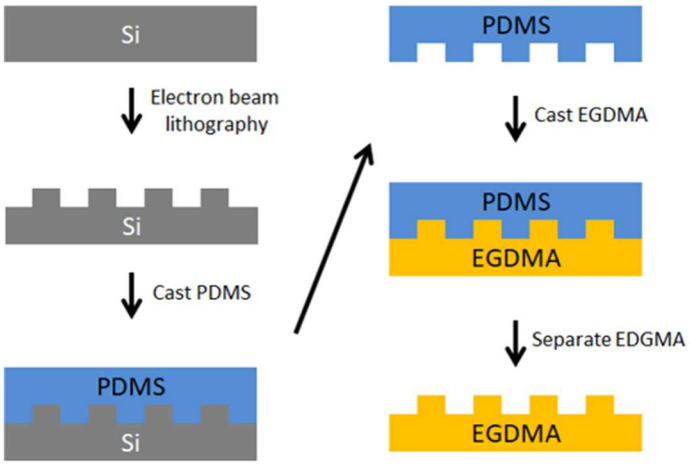

Supplemental 1: Schematic diagram of pattern transfers and EGDMA hydrogel fabrication.

Supplemental 2: Raw data of gap area from ImageJ analysis.

			Time		A0-A24	%Closure
			0h	24h		
Conditions	Control	1	59036	56335	2701	4.6
		2	58468	57220	1248	2.1
		3	55592	51233	4359	7.8
		4	55331	54570	761	1.4
		5	55389	54491	898	1.6
		6	52706	46322	6384	12.1
	Agar (P)	1	58102	38901	19201	33.0
		2	57178	40350	16828	29.4
		3	58713	32360	26353	44.9
		4	57663	41774	15889	27.6
		5	63872	45408	18464	28.9
		6	57481	46305	11176	19.4
	Agar (NP)	1	57519	49937	7582	13.2
		2	56661	46909	9752	17.2
		3	55131	46120	9011	16.3
		4	52868	39110	13758	26.0
		5	55149	41512	13637	24.7
		6	56039	45772	10267	18.3
	PEG (P)	1	60875	11866	49009	80.5
		2	54896	22575	32321	58.9
		3	53079	8360	44719	84.2
		4	57713	2558	55155	95.6
		5	54864	0	54864	100.0
		6	56174	3714	52460	93.4
	PEG (NP)	1	57002	15377	41625	73.0
		2	55155	16679	38476	69.8
		3	56977	13802	43175	75.8
		4	59108	29319	29789	50.4
		5	59995	29393	30602	51.0
		6	58772	16076	42696	72.6

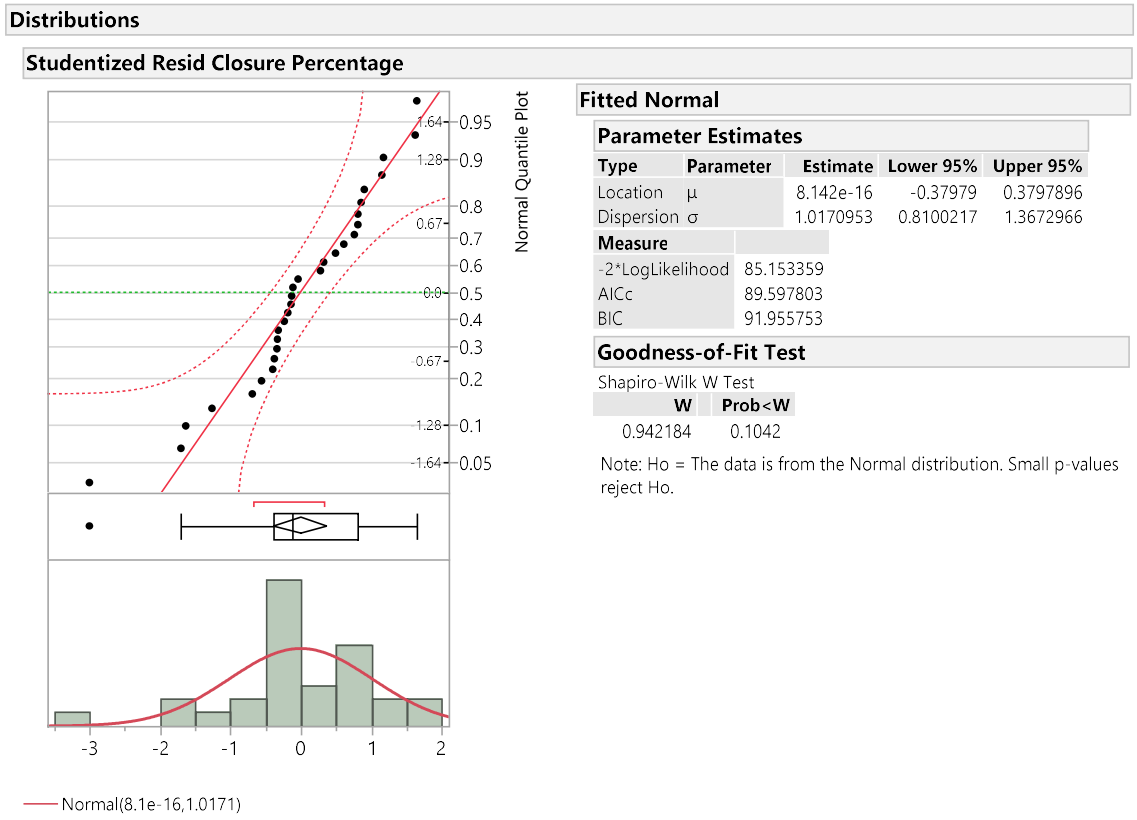

Model Adequacy:

Goodness of fit test indicates the closure rate data is normally distributed.

The points lie close to the diagonal line connecting the 25% and 75% quantiles. The residuals appear to be normally distributed. Therefore, the assumption that closure rate is a normally distributed variable is valid.

Equal variance test:

H_0: The variances within each set are equal ($\sigma_1^2 = \sigma_2^2 = \sigma_3^2 = \sigma_4^2 = \sigma_5^2$)

H_1: The variances are significantly different from each other.

Test	F Ratio	DFNum	DFDen	Prob > F
O'Brien[.5]	1.3875	4	25	0.2669
Brown-Forsythe	1.3220	4	25	0.2891
Levene	2.5167	4	25	0.0668
Bartlett	2.3507	4	.	0.0518

p-value > 0.05 (Do not reject H_0)

Result: The equal variance assumption is valid.

Supplemental 3: Model adequacy tests before conducting ANOVA and Tukey-Kramer evaluations.

Oneway Analysis of Variance of % Closure by Condition

Analysis of Variance

Source	DF	Sum of Squares	Mean Square	F Ratio	Prob > F
Condition	4	26708.373	6677.09	71.2044	<.0001*
Error	25	2344.341	93.77		
C. Total	29	29052.713			

Means for Oneway Anova

Level	Number	Mean	Std Error	Lower 95%	Upper 95%
Agar (NP)	6	19.3016	3.9533	11.16	27.444
Agar (P)	6	30.5447	3.9533	22.40	38.687
Control	6	4.9433	3.9533	-3.20	13.085
PEG (NP)	6	65.4353	3.9533	57.29	73.577
PEG (P)	6	85.4317	3.9533	77.29	93.574

Std Error uses a pooled estimate of error variance

Comparisons for all pairs using Tukey-Kramer HSD: Ordered Differences Report

Level	- Level	Difference	Std Err Dif	Lower CL	Upper CL	p-Value
PEG (P)	Control	80.48843	5.590874	64.0687	96.90812	<.0001*
PEG (P)	Agar (NP)	66.13013	5.590874	49.7104	82.54982	<.0001*
PEG (NP)	Control	60.49198	5.590874	44.0723	76.91167	<.0001*
PEG (P)	Agar (P)	54.88705	5.590874	38.4674	71.30674	<.0001*
PEG (NP)	Agar (NP)	46.13369	5.590874	29.7140	62.55338	<.0001*
PEG (NP)	Agar (P)	34.89060	5.590874	18.4709	51.31029	<.0001*
Agar (P)	Control	25.60138	5.590874	9.1817	42.02107	0.0010*
PEG (P)	PEG (NP)	19.99645	5.590874	3.5768	36.41614	0.0116*
Agar (NP)	Control	14.35830	5.590874	-2.0614	30.77799	0.1074
Agar (P)	Agar (NP)	11.24308	5.590874	-5.1766	27.66277	0.2900

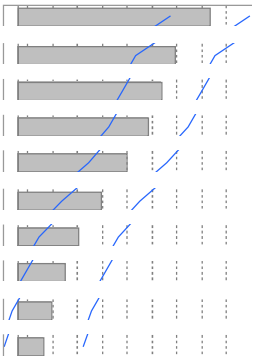

Supplemental 4: Result of One-way ANOVA and post hoc Tukey-Kramer HSD tests.

Comparisons with a control using Dunnett's Method

LSD Threshold Matrix

Level	Abs(Dif)-LSD	p-Value
PEG (P)	65.91	<.0001*
PEG (NP)	45.92	<.0001*
Agar (P)	11.03	0.0004*
Agar (NP)	-0.22	0.0543
Control	-14.6	1.0000

Positive values show pairs of means that are significantly different.

Supplemental 5: Result of Control Dunnett's test.